

Fresh study of simultaneous electron-photon excitation of a Hydrogen atom based on Bethe-Born approximation

Behnam Nikoobakht¹

¹*Theoretische Chemie, Physikalisch-Chemisches Institut,
Universität Heidelberg, INF 229, D-69120 Heidelberg, Germany*

Abstract

The advent of powerful laser sources has made it possible to observe a relatively large cross section of the excited state of Hydrogen atom. This is due to the effect of joint collisions of a linearly polarized N -photon and high-energy electron. For such a process, we evaluate the excitation cross section for geometries, in which the laser field is perpendicular or parallel to the initial momentum of the electron. The second-order, time-dependent perturbation theory together with Bethe-Born approximation suitable for an electron with a large incident energy is employed to obtain the transition amplitude. The amplitudes are calculated for the $S-S$ and $S-D$ transitions of the Hydrogen atom in the Sturmian representation of the non-relativistic Green's function. In particular, we investigate the excitation cross sections for transitions, which have an initial state $1S$ and final state nS with $n \in \{2, 3, 4, 5\}$. The characteristic dependence of the excitation cross section on the momentum of the projectile is shown and discussed. Our investigation indicates that the Bethe-Born approximation yields reasonable results for the excitation cross section of the simultaneous electron photon excitation process when a high energy projectile is treated.

I. INTRODUCTION

The influence of an external magnetic field on atoms was investigated in the Thompson or Rayleigh scattering formulated in the framework of classical electrodynamics [1–3]. This was the first attempt to show the significant effect of the photon field on atomic collisions. This classical result has been confirmed by quantum mechanical treatments, which are also paved the way for the creation of a new class of scattering process involving simultaneous collision of three partners, electron, photon and atom [4]. This collision process belongs to the category of the non-collective processes, in which only three particles are involved in the scattering [4, 5]. The main advantage of this scattering process is to provide a theoretical and experimental base for the study of collective processes including more than three particles interacting simultaneously, such as plasma [6]. Performing a thorough investigation on the non-collective process is required to gain more insight into the collective processes, such as the laser heating of a plasma and laser-driven fusion [7, 8].

In this paper, it is our purpose to study one of the non-collective processes, which is a simultaneous electron-photon excitation (SEPE). For such a process, the excitation cross sections depend on the energy of an incoming electron, the intensity, frequency as well as photon polarization of the laser field [5, 9, 10]. This unique behavior leads to more substantial cross sections than that of the usual excitation process of atomic systems, where the interaction of the electron and atom is only treated in the absence of the laser field [4, 5, 9].

The idea of the SEPE process was innovated by Buimstrov in 1969 [11]. He proposed that if the photon energy of the laser field is not sufficient to excite an atom from its ground state to excited state, an additional free electron may add the energy missing, see Fig. 1. With the advent of powerful laser sources, it has become possible to detect the second-order SEPE process, which has larger excitation cross section than the first-order process [11, 12, 18]. There have been many attempts in order to calculate the excitation cross section of the second-order SEPE process [12, 18]. The authors in Ref. [12] considered a high energy electron (projectile) colliding with a Hydrogen atom in the presence of the laser field. They assumed that the electron and photon energies coincide with the ground and excited state energy difference of the Hydrogen atom [see Eq. (2)]. The authors discussed resonance structures of the excitation cross section of the SEPE process in the second-order

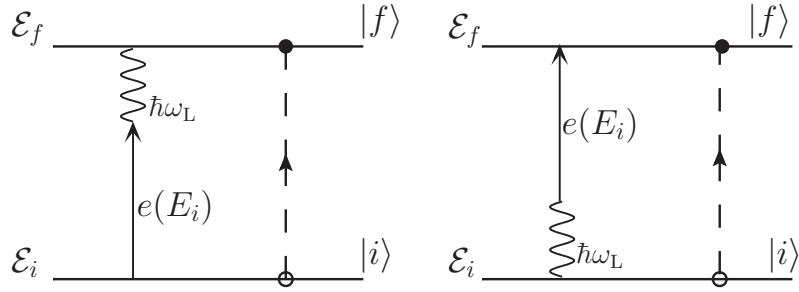


FIG. 1. Schematic representation of the SEPE process. The electron adds the finite value of the energy E_i the photon energy of the laser field ω_L making possible to take place the transition between initial state $|i\rangle$ and final state $|f\rangle$ in a Hydrogen atom.

perturbation theory, where the interactions of the atom with the electron and photon distort the atomic states. The atom-electron interaction was investigated in the framework of the Bethe-Born approximation, where the dipole term of the free electron and the bound-atomic electron interaction gives an important contribution. The atom-photon interaction was dealt with in the dipole approximation, where it was assumed that the wave length of the laser light is large in comparison with the spatial extent of atomic wave functions.

The transition amplitude of the SEPE process presented in Ref. [12] was calculated in the velocity gauge. The result was limited to the transitions between states with the same parity (*i.e.*, S - S transition) for the SEPE process in the Hydrogen atom. In this work, we want to investigate the SEPE process and to go beyond the results presented in Ref. [12]; we first want to obtain analytically the transition amplitude of the SEPE process of the Hydrogen atom for the $S - S$ and $S - D$ transitions. Second, we evaluate numerically the total excitation cross sections of the SEPE process, in which transitions from an initial state to highly excited states are dealt with for two different geometries in our investigation. In Sec. II, we reconsider the SEPE process introduced in Ref. [12] and compute the transition amplitude in the length gauge. As we expect, the same result for the transition amplitude as presented in Ref. [12] is obtained. Going beyond the result of Ref. [12], our finding for the transition amplitude of the second-order SEPE process can be applied for states with different parities ($\Delta l = 0, \pm 2$). Then, we restrict ourselves to transitions with $\Delta l = 0$ (*e.g.* S - S transition) and use the Sturmian representation of the non-relativistic Coulomb Green's

function to evaluate the total cross section of the SEPE process. The analytical results for the radial integral appearing in the evaluation of the total cross sections are presented in Appendix A. In Sec. III, the numerical calculations of the excitation cross sections for the $1S - nS$ transitions, $n \in \{2, 3, 4, 5\}$ induced by the SEPE process for two different geometries are described. In these numerical evaluations, the characteristic dependence of the excitation cross section on the energy of the free electron and on the scattering angle θ for two different geometries is presented and discussed. The effect of the laser orientations with respect to the initial momentum of the free electron on the excitation cross sections is also disputed. We also compare our results with the literature and discuss the reasons for inconsistencies, which are illustrated in Appendix B. Summary and conclusion are given in Sec. IV.

II. GENERAL DESCRIPTION

In this section, we shall give a general description of the excitation of the Hydrogen atom via simultaneous collisions of a high-energy electron with an initial momentum \mathbf{k}_i and a linearly polarized laser field with the frequency ω_L ,

$$e(k_i) + H(n_i) \pm l\hbar\omega_L \rightarrow e(k_f) + H(n_f), \quad (1)$$

where n_i and n_f refer to the principal quantum numbers of the initial and final states in the Hydrogen atom. Note that l is the number of emitted or absorbed photons in this process and k_f is the final momentum of the free electron.

As described in details in Refs. [6, 11], the Hydrogen atom in a joint electron-photon collision is populated in an excited state in the following steps: A free electron with momentum \mathbf{k}_i penetrates the laser field, which is switched on adiabatically (slowly). Then, the electron emits or absorbs l photons and its energy reaches $k_i^2/2m \pm l\hbar\omega_L$. In the next step, the electron interacts with the Hydrogen atom in the initial state and the excitation process takes place. The final energy of the free electron reads,

$$E_f = k_i^2/2m - \Delta\mathcal{E} \pm l\hbar\omega_L, \quad (2)$$

where $\Delta\mathcal{E}$ is the energy difference between the final and initial states. At the final stage, we turn off adiabatically the laser field and the free electron with energy $k_i^2/2m \pm n\hbar\omega_L$ leaves the Hydrogen atom by reabsorption of photons.

As indicated in the previous paragraph, we have used the fact that the time-dependent perturbation is gradually turned on and off. This is the so-called adiabatic switching of the interaction, which allows to avoid the effect of an abrupt change in the Hamiltonian, see Eq. (4) [13]. This allows to replace the time-dependent potential $V(t)$ in the Hamiltonian by $V^{\text{ad}}(t)$,

$$V(t) \rightarrow V^{\text{ad}}(t) = e^{-\eta|t|}V(t), \quad (3)$$

where *ad* refers to the adiabatic picture and η is the damping parameter, which is in the range $0 < \eta < 1$. In the following section, we shall employ the concept of the adiabatic switching of the interaction in the evaluation of the transition amplitude corresponding to the SEPE process of Eq. (1).

A. Evaluation of scattering amplitude

Consider an electron and a plane-wave monochromatic laser field in the z direction colliding simultaneously with a Hydrogen atom in the initial state n_i , as described in Eq. (1). This three-body inelastic scattering is characterized by the following Hamiltonian

$$H = H_0 + V(t), \quad (4)$$

where H_0 refers to the unperturbed Hamiltonian including free electron (projectile) and Hydrogen atom Hamiltonians

$$H_0 = \frac{p_2^2}{2m_e} + \frac{p_1^2}{2m_e} + \frac{Ze^2}{r_1}, \quad (5)$$

where Z is the nuclear charge. The time-dependent interaction term $V(t)$ in Eq. (4) involves two terms,

$$V(t) = \mathcal{V}_1 + \mathcal{V}_2. \quad (6)$$

The first term \mathcal{V}_1 characterizing the interaction of laser field with free and bound electrons is

$$\begin{aligned} \mathcal{V}_1 &= V_1 \sin(\omega_L t) e^{-\eta|t|}, \\ V_1 &= eE\boldsymbol{\epsilon} \cdot (\mathbf{r}_1 + \mathbf{r}_2), \end{aligned} \quad (7)$$

where e , E and ϵ refer to the magnitude of the electric charge, electric field and polarization of electric field, respectively. \mathbf{r}_1 and \mathbf{r}_2 denote the position of the bound and free electrons, respectively. Note that the concept of the adiabatic switching of the time-dependent interaction is considered by the small parameter η in Eq. (7) implying that the time-dependent perturbation of Eq. (7) vanishes at $t \rightarrow -\infty$, then start to increase very slowly to its full value. At the end of the calculation, we let $\eta \rightarrow 0$ to yield the constant intensity result after performing the time integration of the second-order term in the Dyson series [see Eq. (11)]. We now turn our attention to the second term \mathcal{V}_2 of Eq. (6). This term refers to the interaction of the free electron and Hydrogen atom and reads

$$\mathcal{V}_2 = e^2 \left(-\frac{1}{r_2} + \frac{1}{|\mathbf{r}_1 - \mathbf{r}_2|} \right). \quad (8)$$

In the interaction picture, where it is convenient to investigate the SEPE process of Eq. (1), the time-dependent potential is represented by [13, 14]

$$\mathcal{V}_{1,2}^I(t) = \exp\left(\frac{i}{\hbar} H_0 t\right) \mathcal{V}_{1,2}(t) \exp\left(\frac{-i}{\hbar} H_0 t\right) \quad (9)$$

The subscript I refers to the interaction picture, where the kinematical and dynamical evolution of the system are separated. The former one corresponding to the evolution of observable relies on H_0 of Eq. (5), while the latter one corresponding to the evolution of the state vectors is governed by the time-dependent interaction $V^I(t)$ of Eq. (6) [14],

$$i \frac{\partial \phi(t)}{\partial t} = V^I(t) \phi(t). \quad (10)$$

This relation is called Tomonaga-Schwinger equation. Its solution expressed by evolution operator $U_I(\eta, t)$ yields Dyson's perturbation expansion [14]

$$U_I(\eta, t) = 1 - i \int_{-\infty}^{\infty} dt_1 V^I(\eta, t_1) + (-i)^2 \int_{-\infty}^{\infty} dt_1 \int_{-\infty}^{t_1} dt_2 T[V^I(\eta, t_1) V^I(\eta, t_2)] + \dots, \quad (11)$$

where T means a chronological ordering operator. Now, we assume that there is an initial time-dependent state $|\phi_i^I(t)\rangle$ in the interaction picture. Based on the assumption of adiabatic switching of interaction, the wave function in the remote past is free of the laser field effect, *i.e.*, $|\phi_i^I(t \rightarrow -\infty)\rangle = |\phi_i\rangle$, where $|\phi_i\rangle$ is the eigenfunctions of the Hamiltonian of H_0 in Eq. (5). The final state wave function in the interaction picture is generated by the evolution operator $U_I(\eta, t)$ of Eq. (11),

$$\begin{aligned} |\phi_f^I(t)\rangle &= U_I(\eta, t) |\phi_i\rangle = \sum_m c_m(t) |\phi_m\rangle \\ c_m(t) &= \langle m | \phi_f^I(t) \rangle, \end{aligned} \quad (12)$$

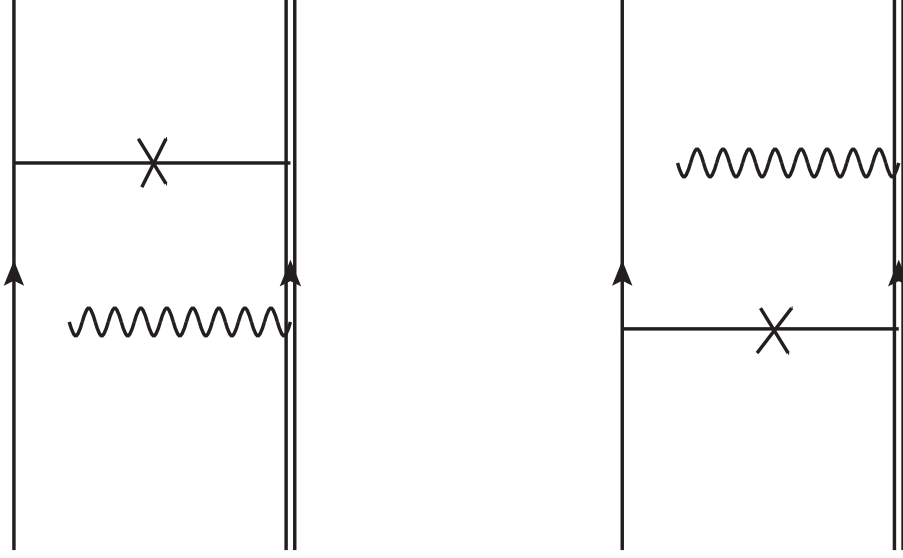


FIG. 2. The corresponding Feynman diagrams to the transition amplitude of laser-assisted inelastic scattering of Eq. (1). The L. H. S diagram is associated with s_{12} and the other one is for s_{21} as indicated Eq. (14). The single and double lines are designated for the free, bound electrons, while the wavy line refers to the photon. The line with cross refers to the interaction between the free electron and the Hydrogen atom.

where $|\phi_f^I(t)\rangle$ is expanded in a complete set $|\phi_m\rangle$ of eigenstates of H_0 . The corresponding transition amplitude to the reference state, $|\phi_f\rangle$, reads

$$c_{\phi_f}^{if} = \langle \phi_f | \phi_f^I(t) \rangle = \langle \phi_f | U_I(\eta, t) | \phi_i \rangle \quad (13)$$

Inserting the evolution operator $U_I(\eta, t)$ of Eq. (11) into Eq. (13) and keeping only the second-order perturbation expansion yields

$$\begin{aligned} c_{\phi_f}^{if} &= \left(-\frac{i}{\hbar}\right)^2 \left[\int_{-\infty}^{\infty} dt_1 \int_{-\infty}^{t_1} dt_2 \langle \phi_f | T[\mathcal{V}_1^I(t_1) \mathcal{V}_2^I(t_2)] | \phi_i \rangle \right. \\ &= \left(-\frac{i}{\hbar}\right)^2 \left[\underbrace{\int_{-\infty}^{+\infty} dt_1 \int_{-\infty}^{t_1} dt_2 \langle \phi_f | \mathcal{V}_1^I(t_1) \mathcal{V}_2^I(t_2) | \phi_i \rangle}_{s_{12}} \right. \\ &\quad \left. \left. + \underbrace{\int_{-\infty}^{+\infty} dt_1 \int_{-\infty}^{t_1} dt_2 \langle \phi_f | \mathcal{V}_2^I(t_1) \mathcal{V}_1^I(t_2) | \phi_i \rangle}_{s_{21}} \right] \right], \quad (14) \end{aligned}$$

where the terms s_{12} and s_{21} are associated with the two Feynman diagrams in Fig. 2 characterizing the second-order SEPE process of Eq. (1). In Eq. (14), the initial and final eigenfunctions $|\phi_{f,i}(r_1, r_2)\rangle$ of the unperturbed Hamiltonian H_0 composed of the product of the free- and bound state-electron wave functions read

$$|\phi_{f,i}(r_1, r_2)\rangle = |\psi_{f,i}(r_1)\rangle \frac{e^{i\mathbf{k}_{f,i}\cdot\mathbf{r}_2}}{(2\pi)^{3/2}}. \quad (15)$$

Here, $\psi_{f,i}(r_1)$ refer to the bound-electron wave functions in the initial and final (excited) states and $k_{f,i}$ refers to the momenta of free electron before and after collision [see Eq. (1)]. Note that the eigenenergy of the Hamiltonian H_0 of Eq. (5) is

$$E_{f,i} = \mathcal{E}_{f,i} + \frac{\hbar^2 k_{f,i}^2}{2m_e}, \quad (16)$$

where the first term denotes the bound electron energy, while the second one refers to the kinetic energy of the incoming and outgoing electrons.

In the following, we concentrate on the evaluation of s_{21} in Eq. (14) corresponding to the R. H. S. diagram in Fig.2. A similar computational method is applied for the evaluation of s_{12} in Eq. (14), which corresponds to the L. H. S. diagram in Fig. 2. Let us rewrite s_{21} in Eq. (14) in terms of the complete set of eigenstates H_0 , including the complete set of bound states $|\phi_m\rangle$ and the continuum of the free-electron states. We get,

$$s_{21} = \left(\frac{-i}{\hbar}\right)^2 \sum_m \int dk_{m'} \int_{-\infty}^{+\infty} dt_1 \int_{-\infty}^{t_1} dt_2 \langle \phi_f | \mathcal{V}_2^I(t_1) | \phi_m \rangle \langle \phi_m | \mathcal{V}_1^I(t_2) | \phi_i \rangle, \quad (17)$$

where $|\phi_m(r_1, r_2)\rangle$ is $|\phi_m\rangle = |\psi_m(r_1)\rangle e^{i\mathbf{k}_{m'}\cdot\mathbf{r}_2}/(2\pi)^{3/2}$. Inserting Eq. (9) into Eq. (17) results in

$$\begin{aligned} s_{21} = & \frac{1}{2\pi^6} \left(\frac{-i}{\hbar}\right)^2 \sum_m \int dk_{m'} \int_{-\infty}^{+\infty} dt_1 \int_{-\infty}^{t_1} dt_2 \\ & \langle \psi_f(r_1) e^{i\mathbf{k}_f\cdot\mathbf{r}_2} | \mathcal{V}_2 | \psi_m(r_1) e^{i\mathbf{k}_{m'}\cdot\mathbf{r}_2} \rangle \times e^{\frac{i}{\hbar}(E_f - E_{mm'})t_2} \times \\ & \times \langle \psi_m(r'_1) e^{i\mathbf{k}_{m'}\cdot\mathbf{r}'_2} | \mathcal{V}_1 | \psi_i(r'_1) e^{i\mathbf{k}_i\cdot\mathbf{r}'_1} \rangle \times e^{\frac{i}{\hbar}(E_{mm'} - E_i)t_1} \end{aligned} \quad (18)$$

Plugging Eq. (7) in Eq. (18) and performing the integration with respect to t_2 yields the

following expression for s_{21} ,

$$\begin{aligned}
s_{21} &= \frac{eE}{(2\pi^2)} \left(\frac{-i}{\hbar}\right)^2 \sum_m \int dk_{m'} \int_{-\infty}^{\infty} dt_1 \times \\
&\times \left(\frac{i\hbar}{E_{mm'} - E_f}\right) \times e^{\eta t_1} e^{\frac{i}{\hbar}(E_f - E_i)t_1} \sin(\omega_L t_1) \times \\
&\times \left\langle \psi_f(r_1) e^{i\mathbf{k}_f \cdot \mathbf{r}_2} \left| \mathcal{V}_2 \right| \psi_m(r_1) e^{i\mathbf{k}_{m'} \cdot \mathbf{r}_2} \right\rangle \times \\
&\times \left\langle \psi_m(r'_1) e^{i\mathbf{k}_{m'} \cdot \mathbf{r}'_2} \left| V_1 \right| \psi_i(r'_1) e^{i\mathbf{k}_i \cdot \mathbf{r}'_1} \right\rangle. \tag{19}
\end{aligned}$$

We convert the sin-term to the exponential terms $e^{-i\omega_L t}$ and $e^{i\omega_L t}$ in Eq. (19). The expression including $e^{-i\omega_L t}$ represents the absorption process in the joint electron-photon collision of Eq. (1), while the other one including $e^{i\omega_L t}$ denotes the emission process associated to Eq. (1). In our calculation, we keep only the absorption part in Eq. (19), *i.e.*, the term involving $e^{-i\omega_L t}$. For emission part, it is sufficient to change the laser frequency sign from $-$ to $+$ in Eqs. (20a)-(20b). After performing the time integration t_1 , s_{21} reads

$$s_{21} = -2\pi i \delta(E_f - E_i - \hbar\omega_L - i\hbar\eta) A_{21}, \tag{20a}$$

$$\begin{aligned}
A_{21} &= \frac{-eE}{(2\pi)^6} \frac{1}{2i\hbar} \sum_m \int dk_{m'} \left\langle \psi_f(r_1) e^{i\mathbf{k}_f \cdot \mathbf{r}_2} \left| \mathcal{V}_2 \right| \psi_m(r_1) e^{i\mathbf{k}_{m'} \cdot \mathbf{r}_2} \right\rangle \\
&\frac{1}{E_f - E_{mm'}} \left\langle \psi_m(r'_1) e^{i\mathbf{k}_{m'} \cdot \mathbf{r}'_2} \left| V_1 \right| \psi_i(r'_1) e^{i\mathbf{k}_i \cdot \mathbf{r}'_2} \right\rangle. \tag{20b}
\end{aligned}$$

In the following, we focus on the evaluation of the matrix elements appearing in Eq. (20b). To do so, we insert Eq. (8) into the first matrix element of Eq. (20b), which reads

$$\begin{aligned}
\left\langle \psi_f(r_1) e^{i\mathbf{k}_f \cdot \mathbf{r}_2} \left| \mathcal{V}_2 \right| \psi_m(r_1) e^{i\mathbf{k}_{m'} \cdot \mathbf{r}_2} \right\rangle &= \frac{4\pi e^2}{|\mathbf{k}_{m'} - \mathbf{k}_f|^2} \times \\
\left\langle \psi_f(r_1) \left| e^{i(\mathbf{k}_{m'} - \mathbf{k}_f) \cdot \mathbf{r}_2} - 1 \right| \psi_m(r_1) \right\rangle. \tag{21}
\end{aligned}$$

Inserting Eq. (7) into the second matrix element of Eq. (20b) yields

$$\begin{aligned}
\left\langle \psi_m(r'_1) e^{i\mathbf{k}_{m'} \cdot \mathbf{r}'_2} \left| V_1 \right| \psi_i(r'_1) e^{i\mathbf{k}_i \cdot \mathbf{r}'_2} \right\rangle &= \\
&= (2\pi)^3 eE \left[\left\langle \psi_m(r'_1) \left| \boldsymbol{\epsilon} \cdot \mathbf{r}'_1 \right| \psi_i(r'_1) \right\rangle \delta^3(\mathbf{k}_i - \mathbf{k}_{m'}) + \right. \\
&\left. \left\langle \psi_m \left| \psi_i \right\rangle \boldsymbol{\epsilon} \cdot \frac{\partial}{i\partial \mathbf{q}'} \delta^3(\mathbf{q}') \right], \tag{22}
\end{aligned}$$

where $\mathbf{q}' = \mathbf{k}_i - \mathbf{k}_{m'}$ and δ refers to the delta function. After substituting Eqs. (21) and (22) in Eq. (20b), the amplitude A_{21} reads

$$A_{21} = \frac{-eE}{(2\pi)^3} \frac{1}{2i\hbar} \sum_m \int dk_{m'} \frac{4\pi e^2}{|\mathbf{k}_{m'} - \mathbf{k}_f|^2} \frac{1}{E_f - E_{mm'}} \left[\left\langle \psi_f(r_1) \left| e^{i(\mathbf{k}_{m'} - \mathbf{k}_f) \cdot \mathbf{r}_1} - 1 \right| \psi_m(r_1) \right\rangle \left\langle \psi_m(r'_1) \left| \boldsymbol{\epsilon} \cdot \mathbf{r}'_1 \right| \psi_i(r'_1) \right\rangle \times \delta^3(\mathbf{k}_i - \mathbf{k}_{m'}) + \left\langle \psi_f(r_1) \left| e^{i(\mathbf{k}_{m'} - \mathbf{k}_f) \cdot \mathbf{r}_1} - 1 \right| \psi_m(r_1) \right\rangle \left\langle \psi_m(r_1) \left| \psi_i(r_1) \right\rangle \boldsymbol{\epsilon} \cdot \frac{\partial \delta^3(\mathbf{q}')}{i\partial \mathbf{q}'} \right]. \quad (23)$$

Eq. (23) is simplified by using the following identity

$$\int \frac{\partial \delta(x)}{\partial x} \phi(x) dx = - \int \delta(x) \frac{\partial \phi(x)}{\partial x} dx. \quad (24)$$

Thus, the amplitude A_{21} is

$$A_{21} = \frac{-eE}{(2\pi)^3} \frac{1}{2i\hbar} \frac{4\pi e^2}{q^2} \sum_m \left\langle \psi_f(r_1) \left| e^{i\mathbf{q} \cdot \mathbf{r}_1} - 1 \right| \psi_m(r_1) \right\rangle \times \frac{1}{E_f - E_{mi}} \left\langle \psi_m(r'_1) \left| \boldsymbol{\epsilon} \cdot \mathbf{r}'_1 \right| \psi_i(r'_1) \right\rangle, \quad (25)$$

where the momentum transfer $\mathbf{q} = \mathbf{k}_i - \mathbf{k}_f$. By using the conservation energy [see Eq. (20a)], the energy denominator in Eq. (25) reads

$$E_f - E_{mi} = \mathcal{E}_i - \mathcal{E}_m + \hbar\omega_L + i\hbar\eta. \quad (26)$$

Thus, the transition amplitude A_{21} is,

$$A_{21} = \frac{-eE}{(2\pi)^3} \frac{1}{2i\hbar} \frac{4\pi e^2}{q^2} \sum_m \frac{\left\langle \psi_f(r_1) \left| e^{i\mathbf{q} \cdot \mathbf{r}_1} - 1 \right| \psi_m(r_1) \right\rangle \left\langle \psi_m(r'_1) \left| \boldsymbol{\epsilon} \cdot \mathbf{r}'_1 \right| \psi_i(r'_1) \right\rangle}{\mathcal{E}_i - \mathcal{E}_m + \hbar\omega_L + i\hbar\eta} \quad (27)$$

A more simplified result can be obtained if we use the Bethe-Born approximation, in which only the leading term of the exponential expression $e^{i\mathbf{q} \cdot \mathbf{r}_1}$ is taken into account ($e^{i\mathbf{q} \cdot \mathbf{r}_1} \simeq 1 + i\mathbf{q} \cdot \mathbf{r}_1$). Therefore, the transition amplitude reads

$$A_{21} = \frac{eE}{(2\pi)^3} \frac{1}{2\hbar} \frac{4\pi e^2}{q^2} \sum_m \frac{\left\langle \psi_f(r_1) \left| \mathbf{q} \cdot \mathbf{r}_1 \right| \psi_m(r_1) \right\rangle \left\langle \psi_m(r'_1) \left| \boldsymbol{\epsilon} \cdot \mathbf{r}'_1 \right| \psi_i(r'_1) \right\rangle}{\mathcal{E}_i - \mathcal{E}_m + \hbar\omega_L + i\hbar\eta}. \quad (28)$$

As mentioned, the same computational method can be utilized to lead the transition amplitude A_{12} . Thus, s_{12} corresponding to the L. H. S. diagram in Fig. 2 reads,

$$s_{12} = -2\pi i \delta(E_f - E_i - \hbar\omega_L - i\hbar\eta) A_{12} \quad (29a)$$

$$A_{12} = \frac{eE}{(2\pi)^3} \frac{1}{2\hbar} \frac{4\pi e^2}{q^2} \sum_m \frac{\langle \psi_f(r_1) | \boldsymbol{\epsilon} \cdot \mathbf{r}_1 | \psi_m(r_1) \rangle \langle \psi_m(r'_1) | \mathbf{q} \cdot \mathbf{r}'_1 | \psi_i(r'_1) \rangle}{\mathcal{E}_f - \mathcal{E}_m - \hbar\omega_L - i\hbar\eta} \quad (29b)$$

Therefore, s_{if} for the process introduced in Eq. (1) is

$$s_{if} = -2\pi i \delta(E_f - E_i - \hbar\omega_L - i\hbar\eta) A_{if}, \quad (30)$$

where A_{if} can be obtained by summing Eqs. (27) and (29b),

$$A_{if} = A_{12} + A_{21} \quad (31a)$$

$$A_{if} = \frac{e^2 E}{(2\pi)^2 q^2 \hbar} \sum_m \left\{ \frac{\langle \psi_f(r_1) | \boldsymbol{\epsilon} \cdot \mathbf{r}_1 | \psi_m(r_1) \rangle \langle \psi_m(r'_1) | \mathbf{q} \cdot \mathbf{r}'_1 | \psi_i(r'_1) \rangle}{\mathcal{E}_f - \mathcal{E}_m - \hbar\omega_L - i\hbar\eta} + \frac{\langle \psi_f(r_1) | \mathbf{q} \cdot \mathbf{r}_1 | \psi_m(r_1) \rangle \langle \psi_m(r'_1) | \boldsymbol{\epsilon} \cdot \mathbf{r}'_1 | \psi_i(r'_1) \rangle}{\mathcal{E}_i - \mathcal{E}_m + \hbar\omega_L + i\hbar\eta} \right\}. \quad (31b)$$

In Eq. (31b), the adiabatic switching of the interaction allows to consider $\eta \rightarrow 0$. The scattering amplitude of Eq. (31b) in a concise form thus reads (in atomic units, $\hbar = m_e = e = 1$)

$$A_{if} = \frac{E}{(2\pi q)^2} \left\{ \langle \psi_f(r_1) | \boldsymbol{\epsilon} \cdot \mathbf{r}_1 \frac{1}{\mathcal{E}_f - H_0 - \hbar\omega_L} \mathbf{q} \cdot \mathbf{r}'_1 | \psi_i(r'_1) \rangle + \langle \psi_f(r_1) | \mathbf{q} \cdot \mathbf{r}_1 \frac{1}{\mathcal{E}_i - H_0 + \hbar\omega_L} \boldsymbol{\epsilon} \cdot \mathbf{r}'_1 | \psi_i(r'_1) \rangle \right\}, \quad (32)$$

It is important to note that Eq. (32) works for both $S - S$ and $S - D$ transitions, while the authors in Ref. [12] obtained the same result for transitions between states with the same parity ($S - S$ transitions).

In Sec. II B, we consider the scattering amplitude A_{if} of Eq. (32) only for the $S - S$ transitions, where the Sturmian representation of the Coulomb Green's function is employed to evaluate analytically the matrix elements appearing in Eq. (32).

B. Scattering amplitude for the $S - S$ transition

In this section, we use the Sturmian representation of the non-relativistic Coulomb Green's function in Eq. (32) to get an explicit form for the scattering amplitude of the

$S - S$ transition. The Schrödinger-Coulomb Green function is defined [15],

$$\frac{1}{\mathcal{E}_{i/f} - H_0 \pm \hbar\omega_L} = \sum_{l,m} g_l(\nu_{i/f}, r, r') Y_{lm}(\Omega) Y_{lm}^*(\Omega'), \quad (33)$$

where the summation is over all possible intermediate states (discrete and continuum states). The symbol Y_{lm} is designated for the spherical harmonics defined in the spherical coordinate system. The function $g_l(\nu, r, r')$ reads [15]

$$g_l(\nu_{i/f}, r, r') = \frac{2m}{\hbar^2} \left(\frac{2}{a_B \nu} \right)^{2l+1} (rr')^l e^{-(r+r')/a_B \nu} \\ \times \sum_{k=0}^{\infty} \frac{k!}{(2l+1+k)!(l+1+k-\nu)} L_k^{2l+1} \left(\frac{2r}{a_B \nu} \right) L_k^{2l+1} \left(\frac{2r'}{a_B \nu} \right), \quad (34)$$

where $L_k^{2l+1}(x)$ refers to the Laguerre polynomial. In the above equation, \hbar and a_B denote Planck constant and Bohr radius, respectively. Note that for simplicity, we drop indexes of r_1 and r'_1 in the rest of our calculation. We exploit the energy parameterization [15]

$$\nu = \frac{Z\hbar}{a_B} \sqrt{-\frac{1}{2m_e E}}, \quad (35)$$

where $E = -(\alpha Z)^2 m_e c^2 / 2n^2$. In Eq. (34), one uses the identity

$$L_k^{2l+1}(x) = \frac{\Gamma(2l+2+k)}{(2l+2)\Gamma(k+1)} {}_1F_1(-k, 2l+2, x) \quad (36)$$

and rewrite Eq.(34) in terms of the confluent Hypergeometric function ${}_1F_1$ and Γ function.

Thus, $g_l(\nu, r, r')$ reads,

$$g_l(\nu, r, r') = \frac{2m}{\hbar^2} \left(\frac{2}{a_B \nu} \right)^{2l+1} (rr')^l e^{-(r+r')/a_B \nu} \\ \times \sum_{k=0}^{\infty} \frac{\Gamma(2l+2+k)[\Gamma(2l+2)]^{-2}}{(l+1+k-\nu)\Gamma(k+1)} {}_1F_1(-k, 2l+2, \frac{2r}{a_B \nu}) {}_1F_1(-k, 2l+2, \frac{2r'}{a_B \nu}) \quad (37)$$

In this position, one can plug Eq. (33) in Eq. (32) and performed the required angular integrations. The scattering amplitude of the $S - S$ transitions induced by SEPE process thus is

$$A_{if} = \frac{E}{(2\pi)q^2} (\mathbf{q} \cdot \boldsymbol{\epsilon}) \frac{a_{if}}{3} \quad (38a)$$

$$a_{if} = \int_0^{\infty} r^3 r'^3 R_{n_f,0}(r) R_{n_i,0}(r') [g_1(\nu_f, r, r') + g_1(\nu_i, r, r')] dr dr' \\ = \frac{4}{9\nu^3} \sum_{k=0}^{\infty} \frac{\Gamma(k+4)}{\Gamma(k+1)(2+k-\nu)} [F_{n_f}(\nu_f) F_{n_i}(\nu_f) + F_{n_f}(\nu_i) F_{n_i}(\nu_i)] \quad (38b)$$

$$F_{n_f/n_i}(\nu_{f/i}) = \int_{k=0}^{\infty} r^4 e^{-\frac{r}{a_B \nu}} {}_1F_1(-k, 4, \frac{2r}{a_B \nu_{f/i}}) R_{n_f/n_i,0}(r) dr \quad (38c)$$

where $R_{n_f,0}(r)$ and $R_{n_i,0}(r)$ are the radial part of the wave function in the ground and excited states. In this investigation, the angular momentum quantum number l of the virtual states in the propagator for the $S - S$ transition is P states.

In Sec. II C, we shall employ the transition amplitude of Eq. (38) in order to evaluate the excitation cross section of the SEPE process of Eq. (1).

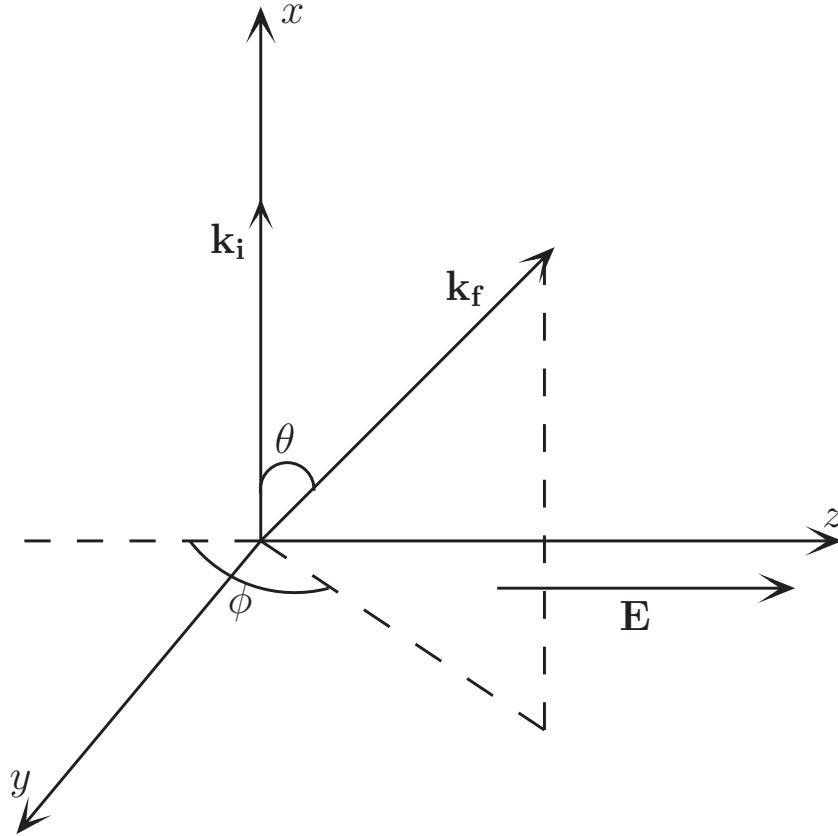


FIG. 3. The electric field \mathbf{E} in the direction of the quantization axis z in the unrotated coordinate system.

C. Total cross section

This section is dedicated to the evaluation of the excitation cross section of the $S - S$ transitions induced by the SEPE process of Eq.(1). The partial cross section in terms of the transition amplitude is defined as follows [13, 14]

$$\frac{d\sigma}{d\Omega} = (2\pi)^4 \frac{k_f}{k_i} |A_{if}|^2. \quad (39)$$

Substituting Eq. (38) into Eq. (39) yields

$$\frac{1}{I_L} \frac{d\sigma}{d\Omega} = 8\pi\alpha \frac{k_f}{k_i} \frac{(\mathbf{q} \cdot \boldsymbol{\epsilon})^2}{q^4} \left| \frac{a_{if}}{3} \right|^2, \quad (40)$$

where $I_L = E^2/8\pi\alpha$ and α is fine structure constant. In the present work, it is assumed that the electric field is the quantization axis [see Fig. 3]. Since it is more convenient to obtain the total cross section in the coordinate system that the transfer momentum \mathbf{q} is the quantization axis, it is required to rotate the coordinate system such a way that \mathbf{q} is the quantization axis in its final status. In this new coordinate system, the components of the electric field unit vector $(\epsilon_0, \epsilon_{\pm 1})$ in the spherical coordinate system are

$$\begin{aligned} \epsilon_0 &= \frac{k_f \cos(\theta_p - \theta) - k_i \cos \theta_p}{q} \\ \epsilon_{\pm 1} &= \frac{-i \sin \theta_p (k_f \cos \theta - k_i) - k_f \cos \theta_p \sin \theta}{\sqrt{2} q}, \end{aligned} \quad (41)$$

where θ is the scattering angle. θ_p refers to the angle between the electric field unit vector (polarization vector $\boldsymbol{\epsilon}$) and the initial momentum of the incoming electron.

Based on the orientation of the electric field with unit vector $\boldsymbol{\epsilon}$ with respect to the initial momentum of the electron \mathbf{k}_i , one can obtain the total cross section for the two special geometries of the joint electron-photon scattering introduced in Eq. (1). Here, we present the analytical results of the total excitation cross sections for the following geometries:

- $\boldsymbol{\epsilon} \perp \mathbf{k}_i$: We consider the case that the electric field is perpendicular to the initial momentum k_i ($\theta_p = \pi/2$). The total cross section for this geometry can be calculated by performing the angular integration in Eq. (40) and reads

$$\frac{\sigma_{\perp}}{I_L} = 8\pi\alpha \frac{k_f}{k_i} A_{\perp} \left| \frac{a_{if}}{3} \right|^2, \quad (42)$$

where A_{\perp} is

$$A_{\perp} = \frac{\pi}{k_i^2} \left[\frac{1}{\chi} \ln \left(\frac{1 + \chi}{1 - \chi} \right) - 2 \right], \quad (43)$$

and χ is defined

$$\chi = \frac{2k_i k_f}{k_i^2 + k_f^2} \quad (44)$$

Here, we should add that there is a deviation between the expression of A_{\perp} and the one in Ref. [12],

$$A'_{\perp} = \frac{\pi}{2k_i^2} \left[\frac{1}{\chi} \ln \left(\frac{1+\chi}{1-\chi} \right) \right]. \quad (45)$$

We have checked our result in Eq. (43). It seems that there is a mistake in Ref. [12], see also Appendix B.

- $\epsilon \parallel \mathbf{k}_i$: We envisage the case that the polarization vector ϵ is parallel to the initial momentum k_i of the electron ($\theta_p = 0$). This assumption leads the following result for the total cross section,

$$\frac{\sigma_{\parallel}}{I_L} = 8\pi\alpha \frac{k_f}{k_i} A_{\parallel} \left| \frac{a_{if}}{3} \right|^2, \quad (46)$$

where A_{\parallel} reads

$$A_{\parallel} = \frac{\pi}{k_i^2} \left[\left(\frac{1}{\chi} - \frac{1}{\varrho} \right) \ln \left(\frac{1+\chi}{1-\chi} \right) + 2 \right], \quad (47)$$

and $\varrho = k_i/k_f$.

III. NUMERICAL RESULTS AND DISCUSSION

This section is dedicated to the numerical evaluations of the cross section of the SEPE process of Eq. (1) for $1S - nS$ transitions, $n \in \{2, 3, 4, 5\}$. Our method is relied on the Schrödinger Coulomb Green function (Sturmian representation of the Green function), which was described in Sec. (IIB). For this investigation, we take into account two different geometries discussed in the previous section. In the numerical calculations presented in this work, we consider the Nd:YAG laser. For the laser frequency and intensity, we use the numerical values introduced in Ref. [18]. According to this reference, the laser frequency ω_L and the laser intensity I_L are 1.17 eV and 10^{13} W/cm², respectively.

TABLE I. Total cross sections in the units of πa_0^2 for the SEPE process of Eq. (1). These values are calculated based on Eq. (42) for $\epsilon \perp \mathbf{k}_i$ geometry. Here, the laser intensity and frequency are $I_L = 10^{13}$ W/cm² and $\omega_L = 1.17$ eV, respectively. We also present total excitation cross sections in absence of laser field.

| Transitions | $E = 100$ eV | | $E = 200$ eV | |
|---------------------|-------------------------|------------------------|-------------------------|------------------------|
| | Laser on | Laser off | Laser on | Laser off |
| $1S \rightarrow 2S$ | 2.6610×10^{-1} | 5.77×10^{-2a} | 1.7173×10^{-1} | 2.95×10^{-2a} |
| $1S \rightarrow 3S$ | 2.8582×10^{-1} | 1.20×10^{-2b} | 1.8869×10^{-1} | 5.99×10^{-3b} |
| $1S \rightarrow 4S$ | 1.9891×10^{-2} | – | 1.0323×10^{-2} | – |
| $1S \rightarrow 5S$ | 1.2356×10^{-3} | – | 8.2514×10^{-4} | – |

^a These values are taken from Ref. [16]

^b These values are taken from Ref. [17]

A. Cross section for $\epsilon \perp k_i$ geometry

The total cross section for the geometry $\epsilon \perp \mathbf{k}_i$ is obtained by using Eq. (42). In this calculation, it is required that the radial integrals and the summation appearing in Eq. (38) are calculated. We perform analytically the radial integrals and the summations for $1S - nS$ transitions(, $n \in \{2, 3, 4, 5\}$) induced by the SEPE process in the Hydrogen atom in appendix A. We emphasize that both discrete and continuum states in the summation appearing in Eq. (38) are treated in our calculations. In table I, for these transitions, the total cross sections are obtained by treating a fast electron with initial energies $E_i = 100$ and 200 eV. We compare one of our results with the available one in the literature [18]. We have found some inconsistencies between our result and the one in the literature. We have devoted appendix B in order to deal with these inconsistencies. In Table I, we also compare some of our results with the excitation cross sections of the inelastic electron-Hydrogen atom scattering in the free field, which were appeared in literature, see *e.g.* Refs. [16, 17]. As we expect, one or two order(s) of magnitude the excitation cross sections induced by the SEPE process is nearly larger than those in the free field, see also Table I.

In the following of our investigation, the behavior of the differential cross section as a function of the scattering angle θ is inspected . It is obtained by taking an integral over the

azimuthal angle ϕ in Eq. (40) leading to

$$\frac{d\sigma}{d\theta} = \int \frac{d\sigma}{d\Omega} d\phi = 16\pi^2 \alpha I_L \frac{k_f}{k_i} \left| \frac{a_{if}}{3} \right|^2 \left[\frac{k_f \sin \theta}{k_i^2 \left(1 + \frac{k_f^2}{k_i^2} - 2 \frac{k_f}{k_i} \cos \theta \right)} \right]^2. \quad (48)$$

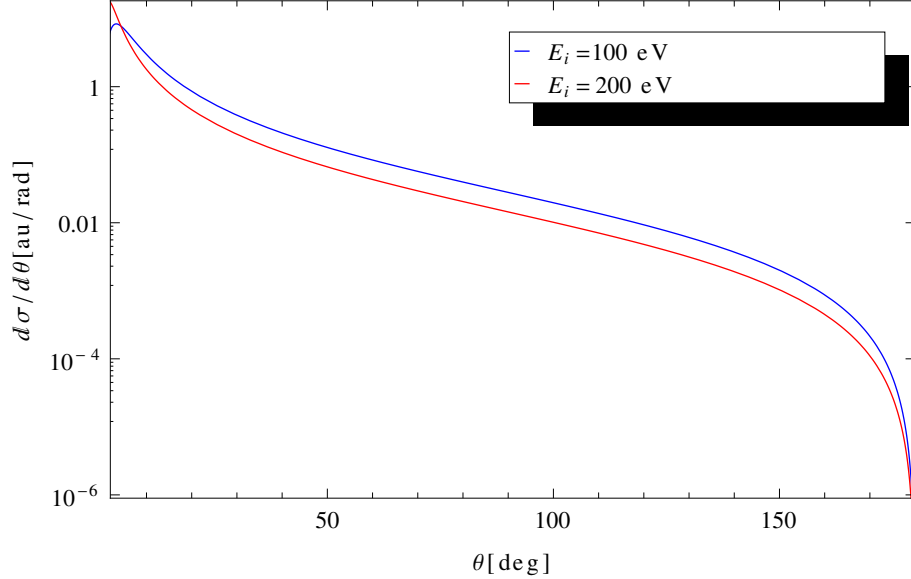


FIG. 4. The behavior of the differential cross section as a function of the scattering angle θ for the $1S - 3S$ transition based on Eq.(48). The initial energy of the electron is assumed to be 100 and 200 eV. The polarization vector of the laser field is perpendicular to the initial momentum of the electron.

In Fig. 4, the behavior of the differential cross section as a function of the scattering angle θ for the free electron with initial energies $E_i = 100$ and 200 eV is compared for the particular case $1S - 3S$ transition. We have also confirmed that the same behaviors for the other transitions $1S - nS$ with $n \in \{2, 4, 5\}$ as presented in Fig. 4 for the $1S - 3S$ transition are observed.

In order to interpret the behavior of the differential cross section of Fig. (4), we consider Eq. (48) in the various ranges of the scattering angle θ . First, we consider the scattering angle θ in the small and intermediate ranges. In these ranges, Eq. (48) can be approximated as follows,

$$\frac{d\sigma}{d\theta} = 16\pi^2 \alpha I_L \frac{k_f}{k_i} \left| \frac{a_{if}}{3} \right|^2 \frac{1}{\beta} \left(\frac{k_i}{k_f} \right)^3 \theta^2, \quad \beta \gg \frac{k_f}{k_i} \theta^2 \quad (49a)$$

$$\frac{d\sigma}{d\theta} = 16\pi^2\alpha I_L \frac{k_f}{k_i} \left| \frac{a_{if}}{3} \right|^2 \frac{1}{\beta} \left(\frac{k_f}{k_i^3} \right) \theta^{-2}, \quad \beta \ll \frac{k_f}{k_i} \theta^2, \quad (49b)$$

where $\beta = (1 - k_f/k_i)^2$. Eq. (49a) indicates that the maximum of $d\sigma/d\theta$ is taking place at very small scattering angle θ and an increase of the initial energy of the electron causes $(d\sigma/d\theta)_{max}$ to move toward zero. This is confirmed by the behavior of the maximum in Fig. 4. For an intermediate scattering angle in Eq. (49b), due to proportionality the differential cross section to θ^{-2} , it is rapidly decreased with increasing the scattering angle θ . This is corroborated by the behavior of $d\sigma/d\theta$ in the intermediate scattering angle of Fig. 4. For large cross section, the differential cross section of Eq. (48) is proportional to $1/\beta$. This means that $d\sigma/d\theta$ does not depend on θ at large scattering angle and it lowers with increasing the initial energy of the free electron E_i . This behavior of the differential cross section is substantiated by Fig. 4 at large scattering angle.

TABLE II. Total cross sections in the units of πa_0^2 for SEPE process of Eq. (1). These values are calculated based on Eq. (46) for $\epsilon \parallel k_i$ geometry. Here, the laser intensity and frequency are $I_L = 10^{13}$ W/cm² and $\omega_L = 1.17$ eV, respectively.

| Transitions | $E = 100$ eV | $E = 200$ eV |
|---------------------|-------------------------|-------------------------|
| $1S \rightarrow 2S$ | 1.1400×10^{-1} | 5.4721×10^{-2} |
| $1S \rightarrow 3S$ | 1.3509×10^{-1} | 6.4666×10^{-2} |
| $1S \rightarrow 4S$ | 9.7101×10^{-3} | 4.6444×10^{-3} |
| $1S \rightarrow 5S$ | 6.1208×10^{-4} | 2.9267×10^{-4} |

B. Cross section for $\epsilon \parallel k_i$ geometry

For this geometry, the total cross section of the SEPE process of Eq. (1) based on Eq. (46) for $1S - nS$ transitions ($n \in \{2, 3, 4, 5\}$) is calculated. We list the total cross sections in the Table II.

In this geometry, the differential cross section as a function of the scattering angle θ is also investigated. It is

$$\frac{d\sigma}{d\theta} = 16\pi^2\alpha I_L \frac{k_f}{k_i} \left| \frac{a_{if}}{3} \right|^2 \left[\frac{1 - (k_f/k_i) \cos \theta}{k_i^2 (1 + (k_f/k_i)^2 - 2(k_f/k_i) \cos \theta)} \right]^2. \quad (50)$$

We draw the differential cross section of Eq. (50) as a function of θ for electrons with initial energies $E_i = 100$ and 200 eV in Fig. 5. In this case, we also pay attention to the

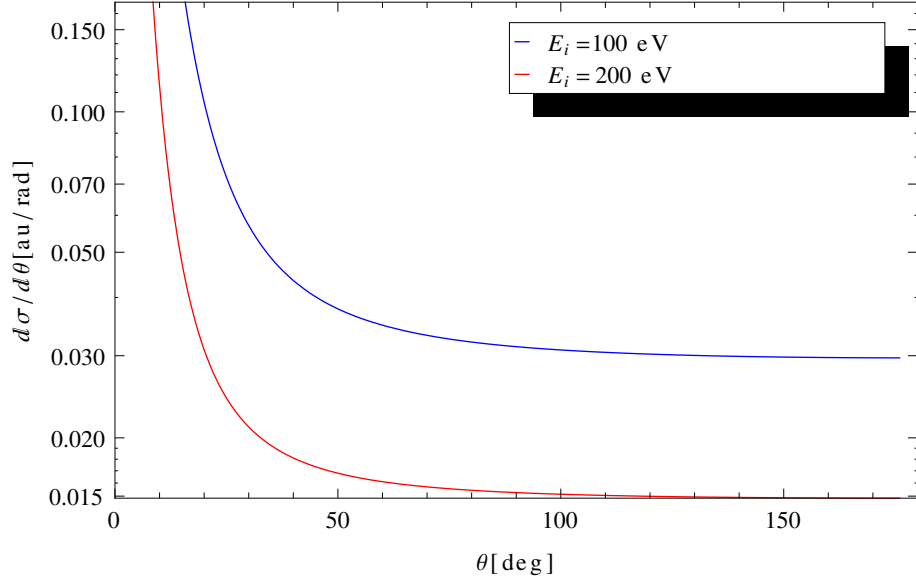


FIG. 5. The behavior of the differential cross section as a function of the scattering angle θ for the $1S - 3S$ transition based on Eq.(50). The polarization vector of the laser field is parallel to the initial momentum of the electron

behavior of $d\sigma/d\theta$ in various regions of the scattering angle. At small and intermediate scattering angles θ , the differential cross sections are

$$\frac{d\sigma}{d\theta} = 16\pi^2 \alpha I_L \frac{k_f}{k_i} \left| \frac{a_{if}}{3} \right|^2 \frac{\beta^{-2}}{k_i^2}, \quad \theta^2 \ll \beta^2 < \beta \quad (51a)$$

$$\frac{d\sigma}{d\theta} = 16\pi^2 \alpha I_L \frac{k_f}{k_i} \left| \frac{a_{if}}{3} \right|^2 \frac{\beta^2 \theta^{-4}}{k_i^2}, \quad \beta^2 \ll \theta^2 < \beta, \quad (51b)$$

Eq. (51a) indicates that the differential cross section is independent of the scattering angle θ at small scattering angle. An increasing energy of the incoming electron leads to a decreasing of the maximum of $d\sigma/d\theta$ at very small scattering angle θ , which is also observed in Fig. 5. For an intermediate scattering angle θ , (see Eq. (51b)), the differential cross section is proportional to $\beta^2 \theta^{-4}/k_i^2$, which describes a rapid decrease of $d\sigma/d\theta$ when the scattering angle is increased. For large scattering angle, it is proportional to $1/2k_i^2$, which shows that

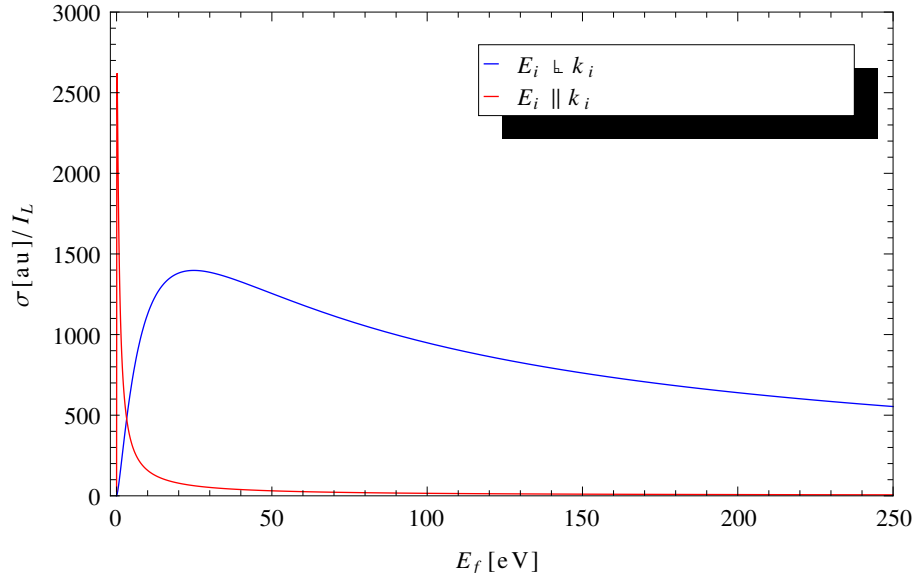


FIG. 6. The total cross section of the $1S - 3S$ transition induced by the SEPE process as function of the final energy of the incident electron for two different geometries.

the differential cross section is independent of the scattering angle and decreases when the energy of the incoming electron is increased.

C. Effect of laser geometry on the cross section

In the following of our investigations, we want to deal with effect of laser beam geometry on the total cross section in the SEPE process. In Fig. 6, we depict the total cross section of the $1S - 3S$ transition as a function of the final energy of the projectile for two different geometries discussed in the previous sections. We have checked that there are the same behaviors for the excitation cross sections of $1S - nS$, with $n \in \{2, 4, 5\}$ as presented in Fig. 6 for the $1S - 3S$ transition.

In Fig. 6, one can observe that the total cross section at low energy projectile tends to zero. Then, for $\epsilon \parallel k_i$ geometry, there is an extremely rapid increase in the total cross section and it starts to fall off very fast as $\ln E/E$. For $\epsilon \perp k_i$ geometry, a moderate increase in the total excitation cross section up to ≈ 25 eV is observed. Then, it starts to fall off as $\ln E/E$ at intermediate and high energies. The existence of logarithmic behavior

in both cases is originated from the fact that the angular momentum is conserved in the atomic collisions in the presence of the laser field [18]. At high energy projectile, where the Bethe-Born approximation works very well, the total cross section for the parallel geometry decreases more rapidly than the perpendicular geometry. As a final remark in Fig. 6 is that an intersection for excitation cross sections for these two different geometries is taken place at low energy part. This may be explained by the fact that the excitation cross section of the SEPE process depends on the projection of the momentum transfer \mathbf{q} on the unit vector of the laser field $\boldsymbol{\epsilon}$, $(\mathbf{q} \cdot \boldsymbol{\epsilon})$. It is always small at high and low energies for the parallel and perpendicular polarization, respectively, see Eqs. (40) and (41). As a consequence, the ratio of $\sigma_{\parallel}/\sigma_{\perp}$ is larger than unit for the low energy part of Fig. 6, while $\sigma_{\parallel}/\sigma_{\perp}$ is less than unit at the high energy part.

IV. SUMMARY AND OUTLOOK

The present study concerns with the theoretical analysis of the second-order SEPE process in the Hydrogen atom, where the photon energy of the laser field and the energy of the electron were assumed to be equal to the atomic state energy difference. The investigation was performed by considering the second-order contribution of Dyson's perturbation series for the evaluation of the excitation cross section induced by the SEPE process. Such a investigation for the second-order SEPE process was discussed earlier in the literature in relation to the appearance of resonance structures in the excitation cross section, where the transition amplitude relation was obtained only for the $S - S$ transition. In the current investigation, we used the dipole and Bethe-Born approximations, where the last one is an appropriate method when high-energy projectile is considered in the SEPE process. The techniques were made possible to evaluate the transition amplitudes for the $S - S$, $S - D$ transitions, see Eq. (32). Total cross sections in the closed forms for two different geometries described are derived in Sec.II. This leads to the characteristic dependency of the excitation cross section on the energy of the projectile (electron) and the scattering angle θ . The total cross sections of $1S - nS, n \in \{2, 3, 4, 5\}$ transitions are obtained. By comparing our results with the ones in the free field, we come to the conclusion that the Bethe-Born approximation generates acceptable results for the SEPE process in the range of high energy projectile (electron).

It is natural to exploit the same idea for the numerical evaluation of the excitation cross section for the $S - D$ transitions induced by the SEPE process in the Hydrogen atom. This extension is left to the future work, and hoped to yield an improved investigation and better understanding of the SEPE process based on the Bethe-Born approximation.

Appendix A: Evaluation of the radial integrals

In this appendix, we give analytical results for radial integrals appearing in Eq. (38), which is a required step for the evaluation of the excitation cross sections of transitions considered in Secs. III A and III B. In general, this radial integral reads

$$a_{if}(\nu) = \int_0^\infty r^3 r'^3 R_{n_f,0}(r) R_{n_i,0}(r') g_1(\nu, r, r') dr dr', \quad (\text{A1})$$

where $g_1(\nu, r, r')$ is defined in Eq. (37). For each transition discussed in text, we obtain the following relations:

$$a_{1S-2S}(v) = \frac{2^9 \sqrt{2}}{3^5 (v^2 - 4)^3 (v^2 - 1)^2 (v^2 + 3v + 2)} \Upsilon_{1S-2S}(v), \quad (\text{A2a})$$

$$\begin{aligned} \Upsilon_{1S-2S}(v) = & 256 + 384v - 416v^2 - 816v^3 - 32v^4 + 360v^5 - 670v^6 - 5\,073v^7 - 6\,037v^8 \\ & - 1\,659v^9 + 65v^{10} + 11\,664v^8 {}_2F_1\left(1, -v; 1 - v; \frac{(v-1)(v-2)}{(v+1)(v+2)}\right). \end{aligned} \quad (\text{A2b})$$

$$a_{1S-3S}(v) = -\frac{3^3 \sqrt{3} v^2}{2^6 (v^2 - 9)^4 (v^2 - 1)^2 (v^2 + 4v + 3)} \Upsilon_{1S-3S}(v), \quad (\text{A3a})$$

$$\begin{aligned} \Upsilon_{1S-3S}(v) = & -59\,049 - 78\,732v + 91\,854v^2 + 148\,716v^3 + 18\,225v^4 - 25\,272v^5 + 303\,588v^6 \\ & + 1\,740\,312v^7 + 1\,767\,177v^8 - 42\,492v^9 - 486\,034v^{10} - 104\,132v^{11} + 2\,639v^{12} \\ & + 131\,072v^8 (-27 + 7v^2) {}_2F_1\left(1, -v; 1 - v; \frac{(v-1)(v-3)}{(v+1)(v+3)}\right). \end{aligned} \quad (\text{A3b})$$

$$a_{1S-4S}(x) = -\frac{2^{14} v^2}{3 \times 5^7 (v^2 - 16)^5 (v^2 - 1)^2 (v^2 + 5v + 4)} \Upsilon_{1S-4S}(v), \quad (\text{A4a})$$

$$\begin{aligned}
\Upsilon_{1S-4S}(v) = & 75\,497\,472 + 94\,371\,840v - 115\,605\,504v^2 - 168\,099\,840v^3 - 29\,196\,288v^4 \\
& + 5\,529\,600v^5 - 492\,011\,520v^6 - 2\,536\,396\,800v^7 - 2\,331\,412\,480v^8 + 479\,833\,600v^9 \\
& + 925\,767\,588v^{10} + 94\,751\,085v^{11} - 76\,666\,371v^{12} - 13426\,985v^{13} + 189\,603v^{14} \\
& + 6\,250\,000v^8(768 - 288v^2 + 23v^4) {}_2F_1\left(1, -v; 1 - v; \frac{(v-1)(v-4)}{(v+1)(v+4)}\right). \quad (\text{A4b})
\end{aligned}$$

$$a_{1S-5S}(x) = -\frac{2^2 5^4 \sqrt{5} v^2}{3^8 (v^2 - 25)^6 (v^2 - 1)^2 (v^2 + 6v + 5)} \Upsilon_{1S-5S}(v), \quad (\text{A5a})$$

$$\begin{aligned}
\Upsilon_{1S-5S}(v) = & -1\,220\,703\,125 - 1\,464\,843\,750v + 1\,855\,468\,750v^2 + 2\,519\,531\,250v^3 \\
& + 519\,531\,250v^4 + 119\,531\,250v^5 + 8\,980\,468\,750v^6 + 43\,557\,656\,250v^7 \\
& + 37\,415\,800\,000v^8 - 12\,363\,971\,250v^9 - 17\,541\,347\,750v^{10} - 471\,962\,250v^{11} \\
& + 2\,213\,557\,150v^{12} + 257\,271\,078v^{13} - 81\,752\,630v^{14} - 12\,080\,802v^{15} + 109\,381v^{16} \\
& + 1\,679\,616v^8(-46\,875 + 20\,625v^2 - 2\,545v^4 + 91v^6) {}_2F_1\left(1, -v; 1 - v; \frac{(v-5)(v-1)}{(v+5)(v+1)}\right). \quad (\text{A5b})
\end{aligned}$$

Note that we use contiguous relations in derivations of above equations [20].

Appendix B: Comparison with literature source

This appendix is devoted to the discussion of the inconsistencies existing between our result for the excitation cross section of the $1S - 2S$ transition induced by the SEPE process and the literature source, see *e.g.*, Ref. [18]. Since we want to find the main reason of inconsistencies between our result and the one presented in Ref. [18], we decided to rederive all equations and results in Ref. [18].

We first rederive the scattering amplitude for $1S - 2S$ transition induced by the SEPE process. We should mention that authors in Ref. [18] used the following form $g_l(\nu_{i/f}, r, r')$ in the Schrödinger-Coulomb green function of Eq. (33) [19],

$$\begin{aligned}
g_l(\nu_{i/f}, r, r') = & -\frac{2(2\nu_{i/f})^{2l+1}}{[(2l+1)!]^2} e^{-\nu_{i/f}(r+r')} (rr')^l \sum_{n=l+1}^{\infty} \left(k - \frac{1}{\nu_{i/f}}\right)^{-1} \frac{(n+l)!}{(n-l-1)!} \times \\
& \times {}_1F_1(l+1-n; 2l+2; 2\nu_{i/f}r) {}_1F_1(l+1-n; 2l+2; 2\nu_{i/f}r'), \quad (\text{B1})
\end{aligned}$$

where ${}_1F_1$ refers to the confluent Hypergeometric function. Note that for simplicity, we drop indexes of r_1 and r'_1 in the rest of our calculation. Putting Eq. (33) into Eq. (32) yields the following formula for the scattering amplitude of the $S - S$ transition induced by the SEPE process,

$$A_{if} = \frac{E}{(2\pi)^2 q^2} \frac{\mathbf{q} \cdot \boldsymbol{\epsilon}}{3} \int r^3 r'^3 R_{n_f,0}^*(r) R_{n_i,0}(r') \left[g_{l=1}(\nu_f, r, r') + g_{l=1}(\nu_i, r, r') \right] dr dr', \quad (\text{B2})$$

where $R_{n_f,0}(r)$ and $R_{n_i,0}(r')$ are the radial part of the wave function in the ground and excited states. Note that $\nu_{i/f} = Z/n_{i/f}$ or $\nu_{i/f} = \mathcal{E}_{i/f} \pm \omega_L$. Inserting Eq. (B1) into Eq. (B2) results in the following relation for the scattering amplitude,

$$A_{if} = \frac{-E}{(2\pi q)^2} \frac{\mathbf{q} \cdot \boldsymbol{\epsilon}}{3} \frac{2^4}{[3!]^2} \left[\nu_f^3 S(\nu_f) + \nu_i^3 S(\nu_i) \right]. \quad (\text{B3})$$

In Eq. (B3), $S(\nu_{i/f})$ reads

$$S(\nu_{i/f}) = \sum_{n=2}^{\infty} n(n^2 - 1) G(n, \nu_{i/f}), \quad (\text{B4})$$

where the summation is over all possible intermediate states. The function $G(n, \nu_{i/f})$ is

$$G(n, \nu_{i/f}) = \left(n - \frac{1}{\nu_{i/f}} \right)^{-1} F_{n_f}(n, \nu_{i/f}) F_{n_i}(n, \nu_{i/f}) \quad (\text{B5a})$$

$$F_{n_{i/f}}(n, \nu_{i,f}) = \int_0^{\infty} r^4 e^{-\nu_{i/f} r} R_{n_{i,f},0}(r) {}_1F_1(2 - n; 4; 2\nu_{i/f} r) dr, \quad (\text{B5b})$$

where $R_{n_{i,f},0}(r)$ is the radial part of the wave function.

Since we are interested in calculating the excitation cross section of the $1S - 2S$ transition induced by the SEPE process based on Eq. (42) (for $\boldsymbol{\epsilon} \perp \mathbf{k}_i$ geometry), it is required to calculate the integrals of Eq. (B5a) for the initial ($n_i = 1$) and final ($n_f = 2$) states. These integrals read,

$$F_{1S}(n, x) = \frac{4!}{(1+x)^6} \left(\frac{1-x}{1+x} \right)^{m-3} (2-nx) \quad (\text{B6a})$$

$$F_{2S}(n, x) = -\frac{12}{\sqrt{2}} \frac{x^2}{(1/2+x)^8} \left(\frac{1/2-x}{1/2+x} \right)^{n-4} \left[n^2 - \left(x + \frac{9}{4x} \right) n + \left(2 + \frac{1}{x^2} \right) \right] \quad (\text{B6b})$$

After inserting Eqs. (B6a) and (B6b) into Eq. (B5a), one can readily calculate $S(\nu_{1S/2S})$ of Eq. (B4),

$$S(\nu_{1S/2S}) = \frac{288x^2}{\sqrt{2}} \sum_{n=2}^{\infty} \frac{n(n^2-1)[n^2 - n(x+9/4) + 1/x^2 + 2]}{n-1/x} \left(\frac{1-x}{1+x}\right)^{n-3} \left(\frac{1/2-x}{1/2+x}\right)^{n-4} \\ \times \frac{2-nx}{(1/2+x)^8(1+x)^6} \quad (\text{B7})$$

This equation should be compared with Eq. (5) from Ref. [18], which is

$$S'(\nu_{1S/2S}) = \frac{256x^2}{3\sqrt{2}} \sum_{n=2}^{\infty} \frac{n(n^2-1)[n^2 - n(x+9/4) + 1/x^2 + 2]}{n-1/x} \left(\frac{1-x}{1+x}\right)^{n-3} \left(\frac{1/2-x}{1/2+x}\right)^{n-4} \\ \times \frac{1}{(1/2+x)^8(1+x)^6} \quad (\text{B8})$$

Clearly, one can observe inconsistencies between Eq. (B7) and Eq. (B8) from Ref. [18]. There is one more reason for the deviation between our numerical result and available literature sources, which is related to Eq. (43). As we discussed in the text, the authors in Refs. [12, 18] employed a wrong expression for A_{\perp} , see Eqs. (43) and (45) [see also Eq. (4a) from Ref. [18] and Eq. (11) from Ref. [12]]. These deviations are responsible for inconsistencies between our numerical result of the excitation cross section of $1S - 2S$ transition and the one in Ref. [18].

Performing summation in Eq.(B7) and inserting it into Eqs. (B3) and (42) yield the total cross section 0.266 in units of πa_0^2 for the $1S - 2S$ transition induced by the SEPE process in Hydrogen atom, which can be compared with the $1S - 2S$ result in Table I. It should be pointed out that this calculation is done for the (electron) projectile with an initial energy 100 eV. We add that the excitation cross section of the $1S - 2S$ transition obtained in Ref. [18] is 1.83 in units of πa_0^2 for the (electron) projectile with energy 100 eV.

-
- [1] Vachaspati, Phys. Rev. **128**, 664 (1962).
 - [2] I. I. Gol'dman, Sov. Phys. JETP **19**, 954 (1964).
 - [3] J. H. Eberly, in: E. Wolf (Ed.), *Progress in Optics Vol. VII*, (North-Holland, Amsterdam, 1969).
 - [4] M. H. Mittleman, *Introduction to the Theory of Laser-Atom Interactions (Physics of Atoms and Molecules) 2nd ed.*, (Plenum Press, New York, 1993).

- [5] F. Ehlötzky, A. Jaroń, J. Z. Kamiński Phys. Rep. **297**, 63 (1998).
- [6] N. J. Mason, Rep. Prog. Phys. **56**, 1275 (1993).
- [7] S. Geltman, J. Res. Natl. Bur. Stand. **82**, 173 (1977).
- [8] K. A. brueckner and S. Jorna, Rev. Mod. Phys. **46**, 325 (1974).
- [9] K. C. Mathur IEEE J. Quant. Elec. **17**, 2233 (1981).
- [10] P. Francken and Y. Attaourti Phys. Rev. A **38**, 1785 (1988).
- [11] V. M. Buimistrov, Phys. Lett. A **30**, 136 (1969).
- [12] N. K. Rahman and F. H. M. Faisal, J. Phys. B **11**, 2003 (1978).
- [13] J. J. Sakurai; San Fu Tuan (Ed.), *Modern Quantum Mechanics Rev. ed.*
(Addison-Wesley, New York, 1994).
- [14] C. J. Joachain, *Quantum Collision Theory, Vol. II*
(North-Holland Publishing Company, Holland 1975).
- [15] R. A. Swainson and G. W. F. Drake, J. Phys. A: Math. Gen **24**, 95 (1991).
- [16] A. E. Kingston, W. C. Fon and P. G. Burke J. Phys. B **9**, 605 (1979).
- [17] A. E. Kingston and J. E. Lauer Proc. Phys. Soc. **88**, 597 (1966).
- [18] N. K. Rahman and F. H. M. Faisal, J. Phys. B **9**, 275 (1976).
- [19] A. Maquet, Phys. Rev. A, **15**, 1088 (1977).
- [20] H. Bateman *Higher Transcendental Functions, Vol. I* (Mcgraw-Hill Book Company, New York 1953).